

Karyotype evolution in *Fusarium*

Cees Waalwijk^{1*}, Masatoki Taga^{2*}, Song-Lin Zheng², Robert H. Proctor³, Martha M. Vaughan³, and Kerry O'Donnell³

¹Businessunit Biointeractions & Plant Health, Wageningen Plant Research, P.O. Box 16, 6700AA, Wageningen, The Netherlands; corresponding author e-mail: cees.waalwijk@wur.nl

²Division of Biological Sciences, Graduate School of Natural Science and Technology, Okayama University, 3-1-1 Tsushima-naka, Kita-ku, Okayama 700-8530, Japan

³Mycotoxin Prevention and Applied Microbiology Research Unit, National Center for Agricultural Utilization Research, Agricultural Research Service, US Department of Agriculture, Peoria, Illinois 61604-3999, USA

*These authors contributed equally to this study

Abstract: The germ tube burst method (GTBM) was employed to examine karyotypes of 33 *Fusarium* species representative of 11 species complexes that span the phylogenetic breadth of the genus. The karyotypes revealed that the nucleolar organizing region (NOR), which includes the ribosomal rDNA region, was telomeric in the species where it was discernible. Variable karyotypes were detected in eight species due to variation in numbers of putative core and/or supernumerary chromosomes. The putative core chromosome number (CN) was most variable in the *F. solani* (CN = 9–12) and *F. buharicum* (CN = 9+1 and 18–20) species complexes. Quantitative real-time PCR and genome sequence analysis rejected the hypothesis that the latter variation in CN was due to diploidization. The core CN in six other species complexes where two or more karyotypes were obtained was less variable or fixed. Karyotypes of 10 species in the *sambucinum* species complex, which is the most derived lineage of *Fusarium*, revealed that members of this complex possess the lowest CN in the genus. When viewed in context of the species phylogeny, karyotype evolution in *Fusarium* appears to have been dominated by a reduction in core CN in five closely related complexes that share a most recent common ancestor (*tricinctum* and *incarnatum-equiseti* CN = 8–9, *chlamyosporum* CN = 8, *heterosporum* CN = 7, *sambucinum* CN = 4–5) but not in the sister to these complexes (*nisikadoi* CN = 11, *oxysporum* CN = 11 and *fujikuroi* CN = 10–12). CN stability is best illustrated by the *F. sambucinum* subclade, where the only changes observed since it diverged from other fusaria appear to have involved two independent putative telomere to telomere fusions that reduced the core CN from five to four, once each in the *sambucinum* and *graminearum* subclades. Results of the present study indicate a core CN of 4 may be fixed in the latter subclade, which is further distinguished by the absence of putative supernumerary chromosomes. Karyotyping of fusaria in the not too distant future will be done by whole-genome sequencing such that each scaffold represents a complete chromosome from telomere to telomere. The CN data presented here should be of value to assist such full genome assembling.

Key words:

accessory
chromosome
genome
NOR
pathogen
phylogeny
qPCR
RPB1
RPB2
supernumerary

Article info: Submitted: 12 January 2018; Accepted: 14 February 2018; Published: 26 February 2018.

INTRODUCTION

The genus *Fusarium* contains over 300 phylogenetically distinct species that occupy a broad array of ecological niches worldwide (Aoki *et al.* 2014). Many of these species are plant pathogens, causing serious diseases on agriculturally, horticulturally and silviculturally important plants, notably *F. graminearum* and *F. oxysporum*, which are ranked among the top five plant pathogenic fungi worldwide (Dean *et al.* 2012). Annually, fusarial diseases are responsible for multi-billion US dollar losses to the world's agricultural economy. In addition, fusaria produce a plethora of mycotoxins, such as trichothecenes, fumonisins and zearalenone, which pose a significant threat to food safety and human health. Toxin contaminated food and feed is frequently unsuitable for consumption, resulting in additional losses to world

agriculture (Munkvold 2017). Phylogenetically diverse fusaria are also capable of causing superficial or invasive, life-threatening opportunistic infections in humans and veterinary animals (O'Donnell *et al.* 2010, 2016). In contrast to most other mycotic agents, fusaria are broadly resistant to the spectrum of antifungals currently available (Guarro 2013, Al-Hatmi *et al.* 2016). Given their global impact on agriculture, and human and veterinary medicine, two web-accessible DNA sequence databases were constructed to facilitate strain typing *via* the internet: FUSARIUM-ID (<http://isolate.fusariumdb.org/>; Geiser *et al.* 2004) and *Fusarium* MLST (<http://www.westerdijkinstituut.nl/fusarium/>; O'Donnell *et al.* 2015).

Comparative phylogenetic and phylogenomic studies have begun to revolutionize our understanding of species limits, evolutionary relationships and mycotoxin potential in *Fusarium*.

© 2018 International Mycological Association

You are free to share - to copy, distribute and transmit the work, under the following conditions:

Attribution: You must attribute the work in the manner specified by the author or licensor (but not in any way that suggests that they endorse you or your use of the work).

Non-commercial: You may not use this work for commercial purposes.

No derivative works: You may not alter, transform, or build upon this work.

For any reuse or distribution, you must make clear to others the license terms of this work, which can be found at <http://creativecommons.org/licenses/by-nc-nd/3.0/legalcode>. Any of the above conditions can be waived if you get permission from the copyright holder. Nothing in this license impairs or restricts the author's moral rights.

Such foundational information is essential for developing novel control strategies aimed at minimizing the threat that fusaria and their toxins pose to agricultural biosecurity. Phylogenetic species recognition based on genealogical concordance (GCPSR *sensu* Taylor *et al.* 2000), which is directed at identifying genealogically exclusive lineages by sequencing portions of several phylogenetically informative loci, has consistently exposed the severe limitations of morphological and biological species recognition in *Fusarium* and greatly accelerated species discovery in the genus. Currently, close to two-thirds of the 300 phylogenetically distinct fusaria were discovered *via* GCPSR studies conducted by scientists worldwide. Phylogenetic analyses of portions of the largest and second largest subunits of RNA polymerase (*RPB1* and *RPB2*) have resolved a monophyletic *Fusarium*, which is strongly supported by the *Fusarium* scientific community (Geiser *et al.* 2013), with 22 clades referred to as species complexes (Laurence *et al.* 2011, O'Donnell *et al.* 2013, Zhou *et al.* 2016).

Following the pioneering *Fusarium* genomics studies by Cuomo *et al.* (2007), Ma *et al.* (2010), and others (reviewed in Ma *et al.* 2013), whole-genome sequences have been obtained from a broad range of fusaria (e.g. Kim *et al.* 2017). To extract full information from the genome, a new standard was proposed, where each contig represents a complete chromosome from telomere to telomere (Waalwijk *et al.* 2017). This approach was elegantly demonstrated for *F. fujikuroi* (Wiemann *et al.* 2013), where each of the 12 scaffolds corresponds to a chromosome. The advantages of a fully assembled genome are multifarious, including a complete inventory of effectors and intact gene clusters as well as structural rearrangements and genomic compartmentalization, as recently reviewed (Thomma *et al.* 2016). In this regard, Ma *et al.* (2010) demonstrated that the genomes of *F. graminearum* and *F. oxysporum* f. sp. *lycopersici* evolved, respectively, by chromosome fusion and acquisition of lineage-specific (LS) chromosomes.

To assist full genome assembling, prior knowledge of chromosome number (CN) of the organism is invaluable. Pulsed field gel electrophoresis (PFGE) has been used extensively since the 1980s to analyse CN in diverse fungi, including *Fusarium* (e.g. Boehm *et al.* 1994, Fekete *et al.* 1993). However, accurate determination of the CN with PFGE is restricted to species that contain small- to intermediate-sized chromosomes such as yeasts because ones larger than 6 Mbp typically cannot be resolved by this technique. Because chromosomes of *Fusarium* and other filamentous fungi are often too large to allow separation by PFGE, their CN has been underestimated in many cases using this technique (Taga *et al.* 1998). Although conventional light-microscopic techniques have been employed historically to determine CN of fungi, most of the published karyotypes of fusaria from this line of research appear to be underestimates (see Table 1). Moreover, these early species identifications without supporting molecular systematic data should be viewed with caution. Fortunately, this technical hurdle was overcome by development (Shirane 1988) and subsequent refinement of the germ tube burst method (GTBM; Taga *et al.* 1998, Tsuchiya & Taga 2001, Mahmoud & Taga 2012), whereby mitotic chromosomes are released from a disrupted

germ tube and spread on a microscope slide, thus enabling accurate chromosome counts. After Taga *et al.* (1998) applied the technique to several species in the *F. solani* species complex, it was used to resolve four chromosomes in *F. graminearum* (Gale *et al.* 2005) and *F. culmorum* (Waalwijk *et al.* 2017) that are too large to be separated by PFGE.

Following the success of the *Fusarium* comparative genomics project (Cuomo *et al.* 2007, Ma *et al.* 2010), powerful platforms for whole-genome sequencing and subsequent assembly and annotation (e.g. CLC Bio Workbench, Aarhus, Denmark) have greatly accelerated progress in fungal genome research over the last decade. In support of these efforts, the present study was initiated to: (1) determine CN for a broad set of *Fusarium* species including representatives of 11 species complexes that span the phylogenetic breadth of the genus; (2) obtain an initial assessment of CN variability in key clades and species; (3) map karyotypes on a robust phylogeny to develop hypotheses of CN evolution; and (4) assess the phylogenetic distribution of putative supernumerary chromosomes within the genus. The results should provide a valuable framework for future comparative phylogenomic research on the genus.

MATERIAL AND METHODS

Material studied

The strains used in this study and the collections in which they are preserved are detailed in Table 1. For convenience in this paper we refer to individual strains by the ARS Culture Collection (<https://nrrl.ncaur.usda.gov/>, NRRL) accession numbers.

Molecular phylogenetic analysis

Strains were grown in 20 mL of yeast-malt broth (YM: 20 g dextrose, 5 g peptone, 3 g yeast extract, and 3 g malt extract per L water; Difco, Detroit, MI) at 25 °C on a rotary shaker set at 200 rpm for 3–5 d. Mycelium was harvested over a Büchner funnel, freeze-dried overnight and then total genomic DNA was extracted from 50–100 mg of pulverized mycelium using a hexadecyltrimethyl-ammonium bromide (CTAB, Sigma-Aldrich, St Louis, MO) protocol (Gardes & Bruns 1993). Portions of the DNA-directed RNA polymerase II largest (*RPB1*) and second largest subunit (*RPB2*) were amplified by PCR and the resulting amplicons were sequenced following published protocols (O'Donnell *et al.* 2010). ABI 3730 sequence chromatograms were edited with Sequencher 5.2.4 (Gene Codes, Ann Arbor, MI) and the aligned consensus sequences were exported as NEXUS files (3383 bp alignment). Maximum likelihood (ML) analyses were conducted with GARLI 2.01 (Zwickl 2006) on the CIPRES Science Gateway TeraGrid (<https://www.phylo.org/>) using the GTR + I + Γ model of molecular evolution. Unweighted maximum parsimony (MP) analyses were conducted with PAUP* 4.0b10 (Swofford 2003), using the heuristic search option, tree bisection-reconnection branch swapping, and 1000 random addition sequences. Clade support was assessed by conducting 1000 ML and MP bootstrap pseudoreplicates of the data (ML-BS/MP-BS). DNA sequences were deposited in GenBank under accession numbers MG282363–MG282421.

Whole-genome sequencing

After total genomic DNA of *F. buharicum* 13371 and *F. subulnatum* 13384 was isolated using a ZR Fungal/bacterial DNA MiniPrep™ kit (Zymo Research, Irvine, CA), genomic DNA libraries were prepared using a NExtera XT DNA library Preparation Kit as specified by the manufacturer (Illumina, San Diego, CA), and then sequence reads were generated using an Illumina MiSeq platform at NCAUR. CLC Genomics Workbench (CLC bio, Qiagen, Aarhus, Denmark) was used to trim and assemble the reads and to analyse the assembled genome sequences.

Cytology

Strains were maintained as slant cultures using synthetic low nutrient agar (SNA, Nirenberg 1976), vegetable juice agar [10 % (v/v) mix vegetable juice (Kagome, Nagoya, Japan), 0.3 % (w/v) CaCO₃, 1.5 % (w/v) agar] or potato dextrose agar (Difco, Detroit, Michigan). The germ tube burst method (GTBM) was used to prepare microscope slides containing mitotic metaphase chromosomes as previously described (Taga *et al.*, 1998, Tsuchiya & Taga 2010, Mehrabi *et al.* 2012). To obtain macroconidia for the GTBM, fusaria were cultured on SNA containing small pieces of filter paper (Aoki & O'Donnell 1999), carnation leaf agar (CLA) (Nelson *et al.* 1983) or mung bean broth (MBB, Gale *et al.* 2005). After macroconidia were harvested, conidia were inoculated in potato dextrose broth (PDB, Difco) according to Taga *et al.* (1998) for strains cultured on SNA and CLA and according to Gale *et al.* (2005) for strains cultured in MBB. To obtain germ tubes, 100–200 µL of a conidial suspension ($3\text{--}5 \times 10^5$ conidia/mL) was placed on a clean slide coated with poly-L-lysine (Sigma-Aldrich P7280, St. Louis, MO) and incubated under humid conditions at 25 °C for 5–12 h until the germ tubes grew to double the length of the macroconidia or the germ tubes began to branch. Of the 44 strains karyotyped, *Fusarium* sp. 22153 FSSC 10 (Fig. 1a) was the only isolate that was treated with thiabendazole to arrest mitosis at metaphase as previously described (Mahmoud & Taga 2012). Once germ tubes had reached the desired length, a 17:3 mixture of methanol and acetic acid was used to burst the germlings and fix their chromosomes. After chromosomes were fixed, they were stained with 4', 6-diamidino-2-phenylindole dihydrochloride (DAPI, Sigma-Aldrich D8417) dissolved in antifade mounting solution (Johnson & Araujo 1981) or Vectashield (Vector Laboratories, Burlingame, CA) at 1 µg/mL. Observations were made using an Olympus BH2 or Olympus BX60 (Olympus, Tokyo, Japan) epifluorescence microscope equipped with a 100X/N.A.1.3 or 1.35 oil immersion objective. Fluorescence images were captured on 400 ASA/ISO colour print film (Fujicolor Super HG400, Fuji Film, Tokyo, Japan) or recorded with a colour CCD camera (DP70, Olympus). Film images were digitized using a COOLSCAN IV ED film scanner (Nikon, Tokyo, Japan).

In filamentous fungi, including *Fusarium*, a thread- or rod-like chromatin protrusion from the apex of a metaphase chromosome has been proven to be nucleolar organizing region (NOR) representing the rDNA region (Taga & Murata 1994, Akamatsu *et al.* 1999, Taga *et al.* 2003). Accordingly we regarded the chromatin protrusion from a chromosome ends observed in this study as NOR (see red arrowheads in Figs 1 and S1).

qPCR experiment

A qPCR experiment was conducted to assess whether the two-fold difference in CN in *F. buharicum* 13371 (CN = 9+1) and *F. subulnatum* 13383 (CN = 18–20) was due to a difference in ploidy. Each strain was grown in YM broth, mycelium was lyophilized and then 30 mg of *F. graminearum* 29169 dry weight mycelium was added as an internal normalizing control to 50 mg of each strain as an internal normalizing control. Genomic DNA was extracted using the ZR Fungal/Bacterial DNA miniprep Kit followed by the Genomic DNA Clean and Concentrate Kit (Zymo Research, Irvine, CA) as prescribed by the manufacturer. The efficiency of qPCR primers targeting translation elongation factor 1- α (*TEF1*; qTEFf: CTCG-GTAAGGGTTCCTTCAAGT × qTEFr: CCAATGACGGTGA-CATAGTAGC) and DNA-directed RNA polymerase II largest subunit (*RPB1*; qRPBf: GTGTTATTCTCAGCCCGCTAT × qRPBb: TCCTTGCTGTCCGTACCATTGA) present in both *F. buharicum* 13371 and *F. subulnatum* 13383, and *Tri6* (*Tri6f*: TAACCACATCGTCGGGACTG × *Tri6r*: GCCGACTTCTT-GCAGGTCTT), which is only present in *F. graminearum* 29169, were determined by generating standard curves from a ten-fold dilution series (50 ng to 0.0005 ng) of mixed DNA for each primer pair. When qPCR was performed, the geometric mean of the two genes Cq values was determined and then normalized to *Tri6* Cq, which allowed the fold-change in copy number of *TEF1* and *RPB1* in 13384 relative to 13371 to be calculated using the $\Delta\Delta Cq$ method (Vandesompele *et al.* 2002, Schmittgen & Livak 2008, Brown *et al.* 2015).

RESULTS

The 44 strains karyotyped in this study were accessioned in the ARS Culture Collection (NRRL), but the acronym is not included with the 5-digit strain number to improve readability. Maximum likelihood and maximum parsimony bootstrapping (ML-BS/MP-BS) of the 108 taxon partial *RPB1* + *RPB2* datasets (3383 bp) were conducted, respectively, with GARLI (Zwickl 2006) and PAUP* (Figs 1, S1). Phylogenies inferred for the 104 fusaria comprising the in-group were rooted on sequences of *Neonectria* and *Ilyonectria* based on more inclusive analyses (O'Donnell *et al.* 2013). Forty-six of the nodes received ≥ 90 % ML-BS/MP-BS support (identified by thickened black nodes), including representatives of 20 species complexes that were strongly supported as monophyletic. However, the eight nodes in red along the backbone of the phylogenies received < 70 % ML-BS/MP-BS (Figs 1 and S1).

The germ tube burst method with DAPI staining (Taga *et al.* 1998) was used to determine the chromosome number for 33 fusaria representing 11 species complexes.

When the nucleolar organizing region (NOR) representing the amplified rDNA region was visible, it was always telomeric on one chromosome as reported by Taga *et al.* (1998, see red arrowheads in Figs 1 and S1). Putative supernumerary chromosomes were detected in 19 species spanning 11 species complexes. These were indicated with yellow arrowheads and the number following the + sign on the images in the left panel (Figs 1, S1). The CNs are described as the number of putative core chromosomes + putative supernumerary chromosomes such as 10+1. The latter were

Table 1. *Fusarium* isolates used in this study with the chromosome (CN) numbers found.

Species Complex ¹	Figure	<i>Fusarium</i> Species ²	NRRL ³	Alternative accession nos ⁴	CN ⁵	Core Chromosomes	Non-core Chromosomes
<i>dimerum</i>	Fig. 1a	<i>F. dimerum</i>	20691	CBS 489.81	15	13	2
<i>dimerum</i>	Fig. S1a	<i>F. dimerum</i>	36130	CBS 102613	15	13	2
<i>ventricosum</i>	Fig. 1a	<i>F. ventricosum</i> -2	25729	CBS 430.91	11	10	1
<i>ventricosum</i>	Fig. S1a	<i>F. ventricosum</i> -1	13953	CBS 830.85	11-15	10 or 11	1, 3 or 4
<i>solani</i>	Fig. 1a	<i>Fusarium</i> sp. FSSC 11	66287	ATCC 204495	15	12	3
<i>solani</i>	Fig. S1a	<i>Fusarium</i> sp. FSSC 11	66287	ATCC 204495	15	12	3
<i>solani</i>	Fig. 1a	<i>F. striatum</i>	22147	BBA 64379	13	12	1
<i>solani</i>	Fig. S1a	<i>F. striatum</i>	22101	BBA 64379	12	12	0
<i>solani</i>	Fig. 1a	<i>Fusarium</i> sp. FSSC 10	22153	ATCC 18099	9	9	0
<i>solani</i>	Fig. S1a	<i>Fusarium</i> sp. FSSC 10	22165	ATCC 18098	10	9	1
<i>buharicum</i>	Fig. 1b	<i>F. sublunatum</i>	13384	CBS 189.34 = BBA 62431	18-20	18-20	0
<i>buharicum</i>	Fig. S1b	<i>F. sublunatum</i>	13384	CBS 189.34 = BBA 62431	18-20	18-20	0
<i>buharicum</i>	Fig. 1b	<i>F. buharicum</i>	13371	CBS 796.70 = DSM 62165 = FRC R-4955	10	9	1
<i>buharicum</i>	Fig. S1b	<i>F. buharicum</i>	13371	CBS 796.70 = DSM 62165 = FRC R-4955	10	9	1
<i>lateritium</i>	Fig. 1b	<i>F. stilboides</i>	20429	ATCC 15662	15	14	1
<i>lateritium</i>	Fig. S1b	<i>F. stilboides</i>	20429	ATCC 15662	15	14	1
<i>nisikadoi</i>	Fig. 1b	<i>F. nisikadoi</i>	25203	MAFF 237507 = BBA 69014	11	10	1
<i>nisikadoi</i>	Fig. S1b	<i>F. nisikadoi</i>	25308	MAFF 237506	12	11	1
<i>fujikuroi</i>	Fig. 1b	<i>F. nygamai</i>	66293	FRC M-7492	12	12	0
<i>fujikuroi</i>	Fig. S1b	<i>F. nygamai</i>	66291	FRC M-5868	12	13	2
<i>fujikuroi</i>	Fig. 1b	<i>F. verticillioides</i>	66290	MAFF 239106	11	10	1
<i>fujikuroi</i>	Fig. S1b	<i>F. verticillioides</i>	66290	MAFF 239106	11	10	1
<i>fujikuroi</i>	Fig. 1b	<i>F. proliferatum</i>	66289	ITEM 2287	12	10	2
<i>fujikuroi</i>	Fig. S1b	<i>F. proliferatum</i>	36220	CBS 115.97	13	11	2
<i>fujikuroi</i>	Fig. 1b	<i>F. fujikuroi</i>	66288	MAFF 238524	12	11	1
<i>fujikuroi</i>	Fig. S1b	<i>F. fujikuroi</i>	66292	MAFF 238525	12	11	1
<i>heterosporum</i>	Fig. 1c	<i>F. heterosporum</i>	20693	CBS 720.79 = PD 79/878	8	7	1
<i>heterosporum</i>	Fig. S1c	<i>F. heterosporum</i>	20693	CBS 720.79 = PD 79/878	8	7	1
<i>heterosporum</i>	Fig. 1c	<i>F. graminum</i>	20692	CBS 737.79 = BBA 62228	7	7	0
<i>heterosporum</i>	Fig. S1c	<i>F. graminum</i>	20692	CBS 737.79	7	7	0
<i>tricinctum</i>	Fig. 1c	<i>F. tricinctum</i>	25481	CBS 393.93 = BBA 64485	9	8	1
<i>tricinctum</i>	Fig. S1c	<i>Fusarium</i> sp.	36132	CBS 102796	10	9	1
<i>tricinctum</i>	Fig. 1c	<i>F. acuminatum</i>	28652	ITEM 865	10	9	1
<i>tricinctum</i>	Fig. S1c	<i>F. acuminatum</i>	28449	CBS 214.77	9	8	1
<i>tricinctum</i>	Fig. 1c	<i>F. arthrosporioides</i>	26416	CBS 303.95	11	8	3
<i>tricinctum</i>	Fig. S1c	<i>F. arthrosporioides</i>	26416	CBS 303.95	11	8	3
<i>tricinctum</i>	Fig. 1c	<i>F. avenaceum</i>	36374	CBS 239.94 = IPO 92-3 = PD 92/1185	9	8	1
<i>tricinctum</i>	Fig. S1c	<i>F. avenaceum</i>	26911	CBS 408.86 = FRC R-8510	10	8	2
<i>incarnatum-equiseti</i>	Fig. 1c	<i>Fusarium</i> sp. FIESC 24	36255	CBS 145.44 = BBA 4095	9	8	1
<i>incarnatum-equiseti</i>	Fig. S1c	<i>Fusarium</i> sp. FIESC 24	36255	CBS 145.44 = BBA 4095	9	8	1
<i>incarnatum-equiseti</i>	Fig. 1c	<i>Fusarium</i> sp. FIESC 16	20425	CBS 131.73 = IMI 160602	9	9	0
<i>incarnatum-equiseti</i>	Fig. S1c	<i>Fusarium</i> sp. FIESC 16	20425	CBS 131.73 = IMI 160602	9	9	0
<i>sambucinum</i>	Fig. 1d	<i>F. longipes</i> -4	13317	FRC R-314	5	5	0
<i>sambucinum</i>	Fig. S1d	<i>F. longipes</i> -4	13317	FRC R-314	5	5	0
<i>sambucinum</i>	Fig. 1d	<i>F. cf. compactum</i>	13829	FRC R-6784	5	5	0

Table 1. (Continued).

Species Complex ¹	Figure	<i>Fusarium</i> Species ²	NRRL ³	Alternative accession nos ⁴	CN ⁵	Core Chromosomes	Non-core Chromosomes
<i>sambucinum</i>	Fig. S1d	<i>F. cf. compactum</i>	13829	FRC R-6784	5	5	0
<i>sambucinum</i>	Fig. 1d	<i>F. poae</i>	66297	TAPO 21	6	4	2
<i>sambucinum</i>	Fig. S1d	<i>F. poae</i>	66297	TAPO 21	6	4	2
<i>sambucinum</i>	Fig. 1d	<i>F. kyushuense</i>	66296	MAFF 240372	4	4	0
<i>sambucinum</i>	Fig. S1d	<i>F. kyushuense</i>	66296	MAFF 240372	4	4	0
<i>sambucinum</i>	Fig. 1d	<i>F. sporotrichioides</i>	66295	ITEM 3593	6	5	1
<i>sambucinum</i>	Fig. S1d	<i>F. sporotrichioides</i>	66295	ITEM 3593	6	5	1
<i>sambucinum</i>	Fig. 1d	<i>F. pseudograminearum</i>	28065	CBS 109954 = FRC R-6761	4	4	0
<i>sambucinum</i>	Fig. S1d	<i>F. pseudograminearum</i>	28065	CBS 109954 = FRC R-6761	4	4	0
<i>sambucinum</i>	Fig. 1d	<i>F. lunulosporum</i>	13393	BBA 62459 = FRC R-5822	4	4	0
<i>sambucinum</i>	Fig. S1d	<i>F. lunulosporum</i>	13393	BBA 62459 = FRC R-5822	4	4	0
<i>sambucinum</i>	Fig. 1d	<i>F. cerealis</i>	13721	CBS 110268 = KF-748	4	4	0
<i>sambucinum</i>	Fig. S1d	<i>F. cerealis</i>	25491	CBS 589.93	4	4	0
<i>sambucinum</i>	Fig. 1d	<i>F. culmorum</i>	66294	IPO 39	4	4	0
<i>sambucinum</i>	Fig. S1d	<i>F. culmorum</i>	66294	IPO 39	4	4	0
<i>sambucinum</i>	Fig. 1d	<i>F. graminearum</i>	31084	PH-1	4	4	0
<i>sambucinum</i>	Fig. S1d	<i>F. graminearum</i>	38154	Fg820	4	4	0

¹As defined in O'Donnell *et al.* (2013).

²Phylogenetic species within the *Fusarium solani* (FSSC) and *F. incarnatum-equiseti* (FIESC) species complexes are distinguished by a unique Arabic number. *Fusarium* sp. FSSC 11 was previously reported as *F. solani* f. sp. *pisi* (VanEtten *et al.* 1994), but *F. solani* corresponds to phylospecies FSSC 5 (Schroers *et al.* 2016). In addition, phylogenetically distinct species within the *F. ventricosum* and *F. longipes* clades are identified by unique numbers.

³NRRL, ARS Culture Collection, Peoria, IL.

⁴ATCC, American Type Culture Collection, Manassas, VA; BBA, Biologische Bundesanstalt für Land-und Forstwirtschaft, Berlin, Germany; CBS, Westerdijk Fungal Biodiversity Institute, Utrecht, The Netherlands; DSMZ, Leibniz-Institut DSMA-Deutsche Sammlung von Mikroorganismen und Zellkulturen, Braunschweig, Germany; FRC, Fusarium Research Center, The Pennsylvania State University, State College, PA; IMI, CABI Biosciences, Egham, Surrey, UK; IPO, IPO-Collection of Fungal Pathotypes, Wageningen, The Netherlands; ITEM, Agro-Food Microbial Culture Collection, Bari, Italy; KF, Fusarium collection at the Institute of Plant Genetics, Polish Academy of Sciences, Poznan, Poland; Institute of Food Technology Culture Collection, Agricultural University of Poznan, Poland; MAFF, Genbank Project, Ministry of Agriculture, Forestry and Fisheries, Tsukuba, Japan; PD, Dutch Plant Protection Service, Wageningen, The Netherlands; TAPO, Agricultural Biotechnology Center, Gödöllő, Hungary.

⁵CN, chromosome number.

defined based on estimated sizes < 2 Mb consistent with prior comparative genomic analyses of phylogenetically diverse fusaria (Coleman *et al.* 2009, Ma *et al.* 2010).

***Fusarium ventricosum* and *F. dimerum* species complexes**

The *Fusarium ventricosum* and *F. dimerum* clades represent the two earliest diverging lineages of *Fusarium*. The CN of two phylospecies, *F. ventricosum*-2 25729 and *F. ventricosum*-1 13953, were 10+1 (Fig. 1a) and 10+1-to-11+4 (Fig. S1a), respectively. *Fusarium ventricosum*-1 13953 was the only strain karyotyped where variable numbers of core and supernumerary chromosomes were detected (i.e., 11(10+1), 14(11+3) and 15(11+4)). *Fusarium dimerum* strains 20691 (Fig. 1a) and 36130 (Fig. S1a) both possessed 13 core and two putative supernumerary chromosomes (i.e., 13+2).

***Fusarium solani* species complex (FSSC)**

Two unnamed phylospecies within this large species complex were analysed (i.e. FSSC 10 and 11, O'Donnell *et*

al. 2008). *Fusarium* sp. FSSC 10 (formerly *F. solani* f. sp. *cucurbitae* and *Nectria haematococca* MPI) strains 22153 and 22165 contained 9 and 9+1 chromosomes, respectively (Figs 1a and S1a). By way of contrast, *F. striatum* FSSC 21 strain 22147 contained 12 and 22101 12+1 chromosomes. *Fusarium* sp. phylospecies FSSC 11 (formerly *F. solani* f. sp. *pisi* and *N. haematococca* MPVI) strain 66287 contained 12+3 chromosomes (Figs 1a and S1a).

***Fusarium buharicum* species complex**

Two species in this complex, *F. buharicum* and *F. sublunatum*, were karyotyped. The CN of *F. buharicum* 13371 was 9+1. However, in marked contrast, the CN of the closely related species *F. sublunatum* 13384 was 18 to 20 (Figs 1b, S1b). To investigate the possible cause(s) of the differences in the karyotype of *F. buharicum* 13371 and *F. sublunatum* 13384, we generated whole-genome sequence data, which indicated the genome of *F. sublunatum* 13384 was 35.7 Mb (N50 = 102.3 kb) and *F. buharicum* 13371 36.1 Mb (N50 = 61.4 kb). The similar genome sizes of the two species indicate the larger number of

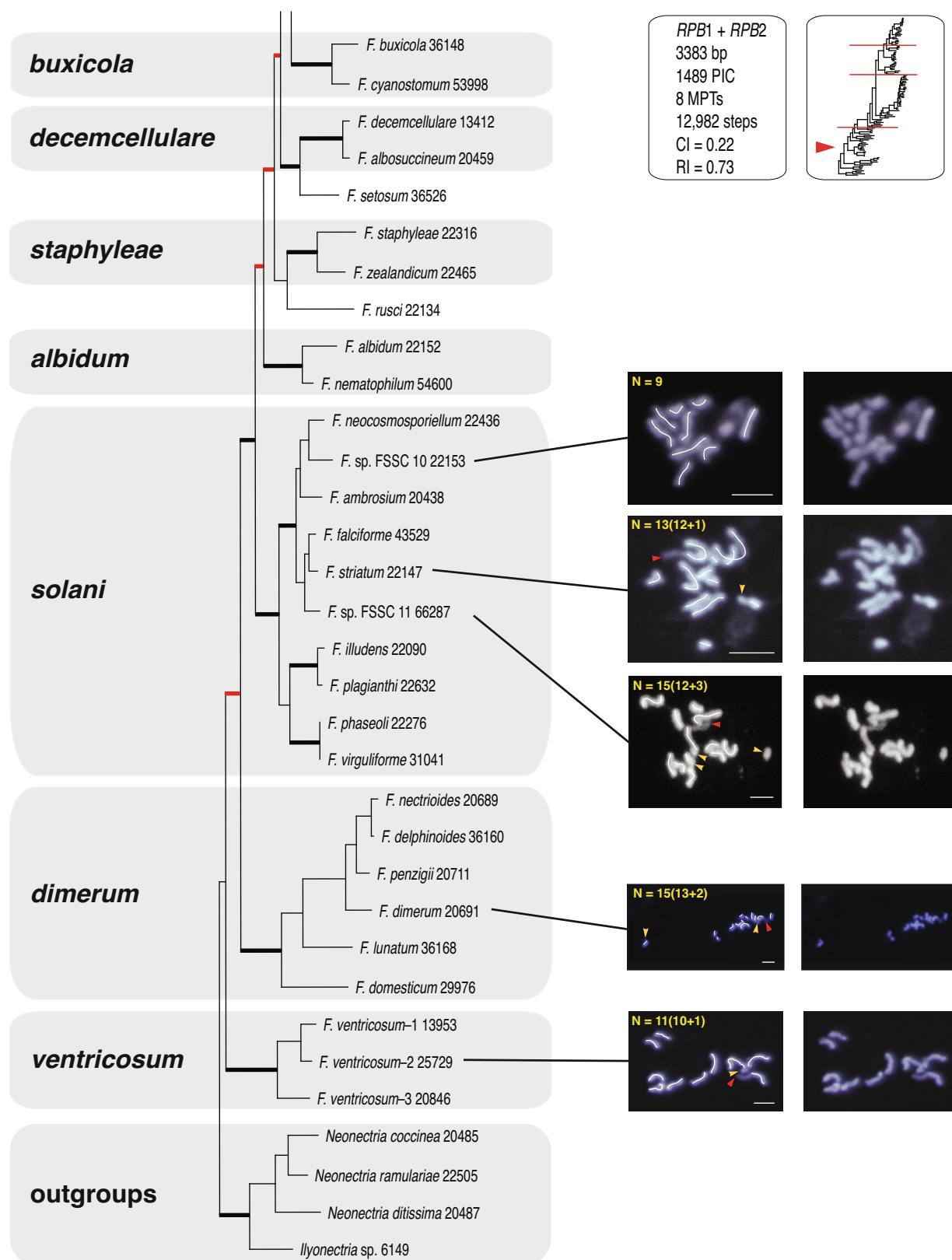
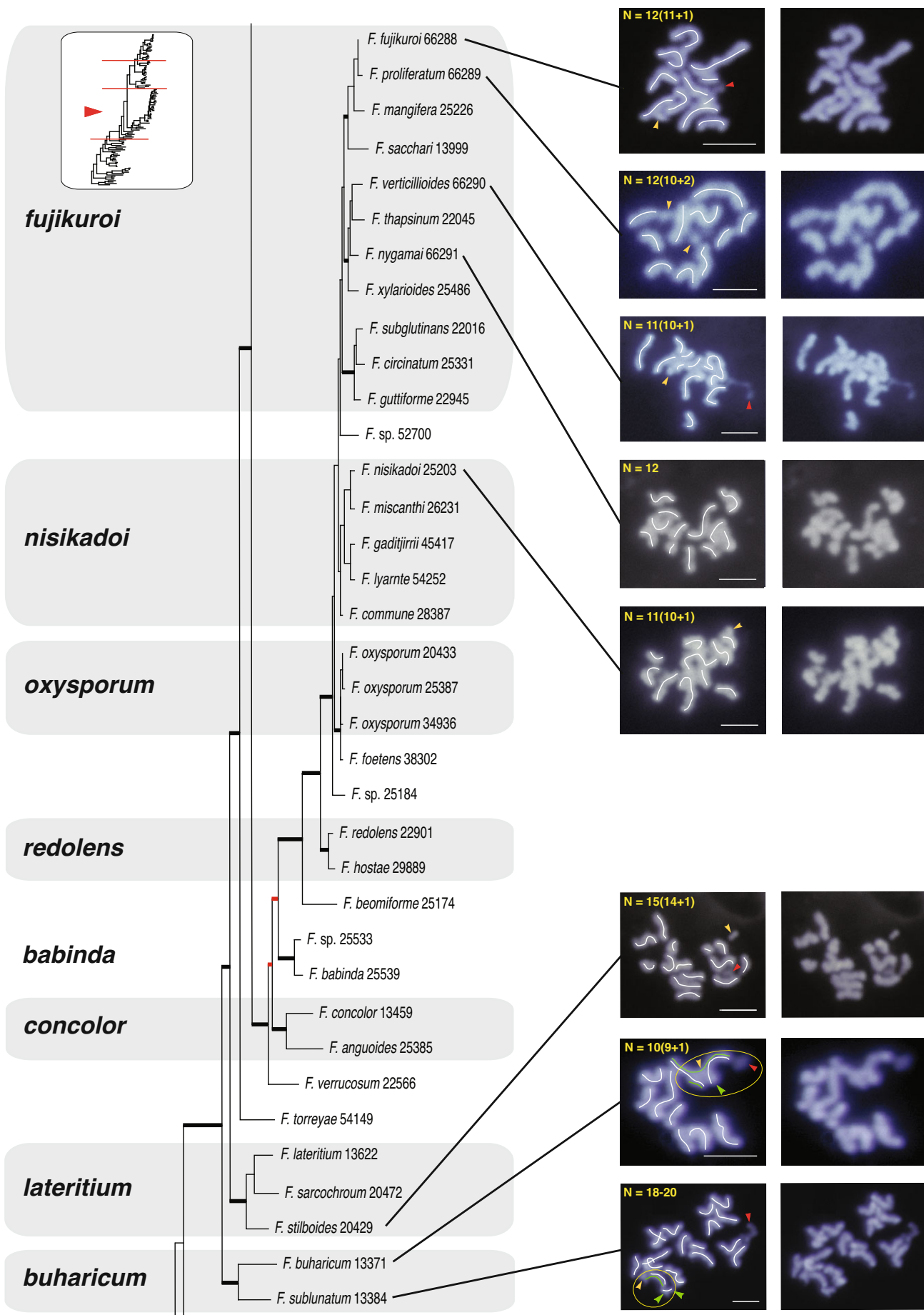
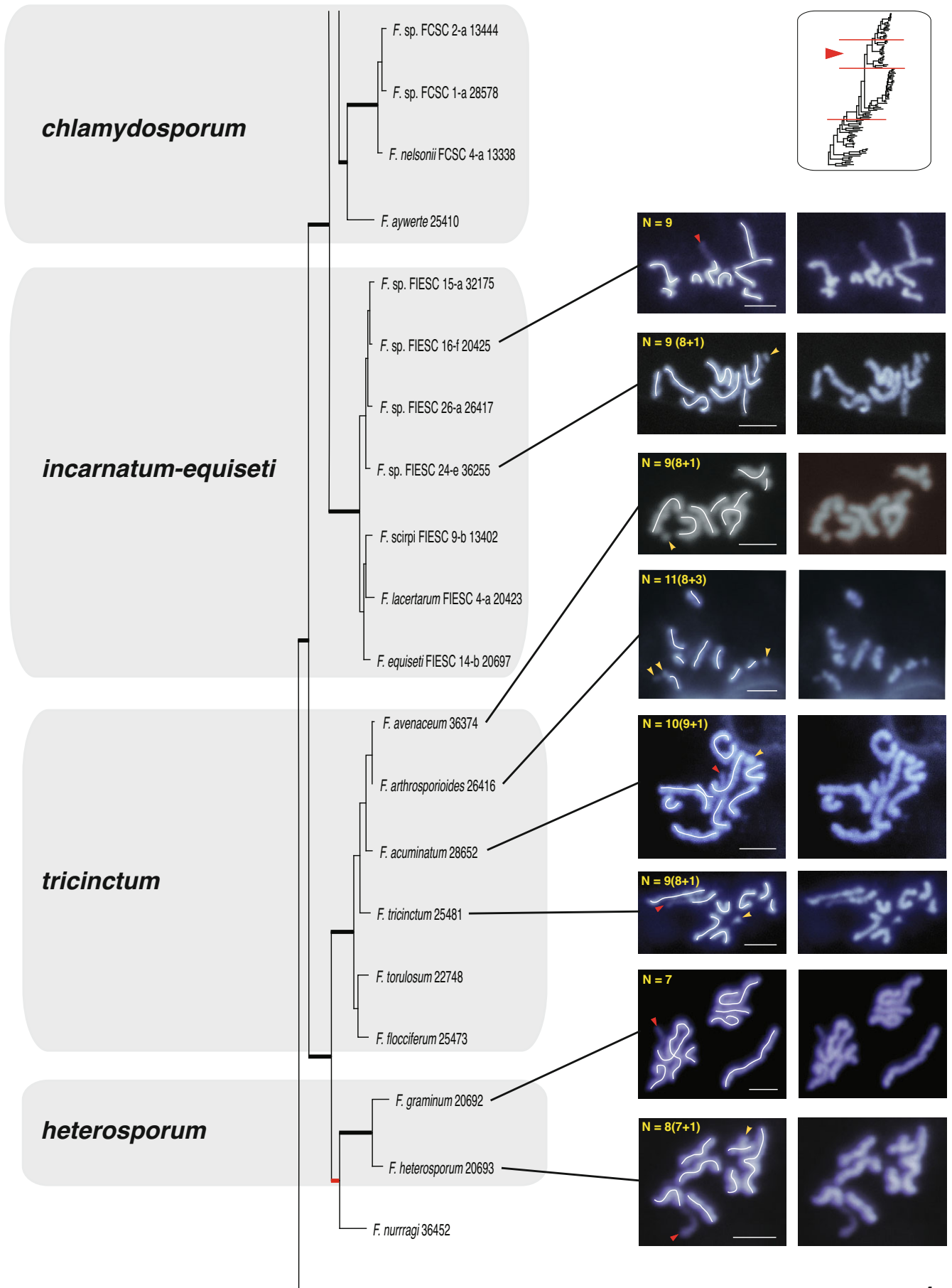


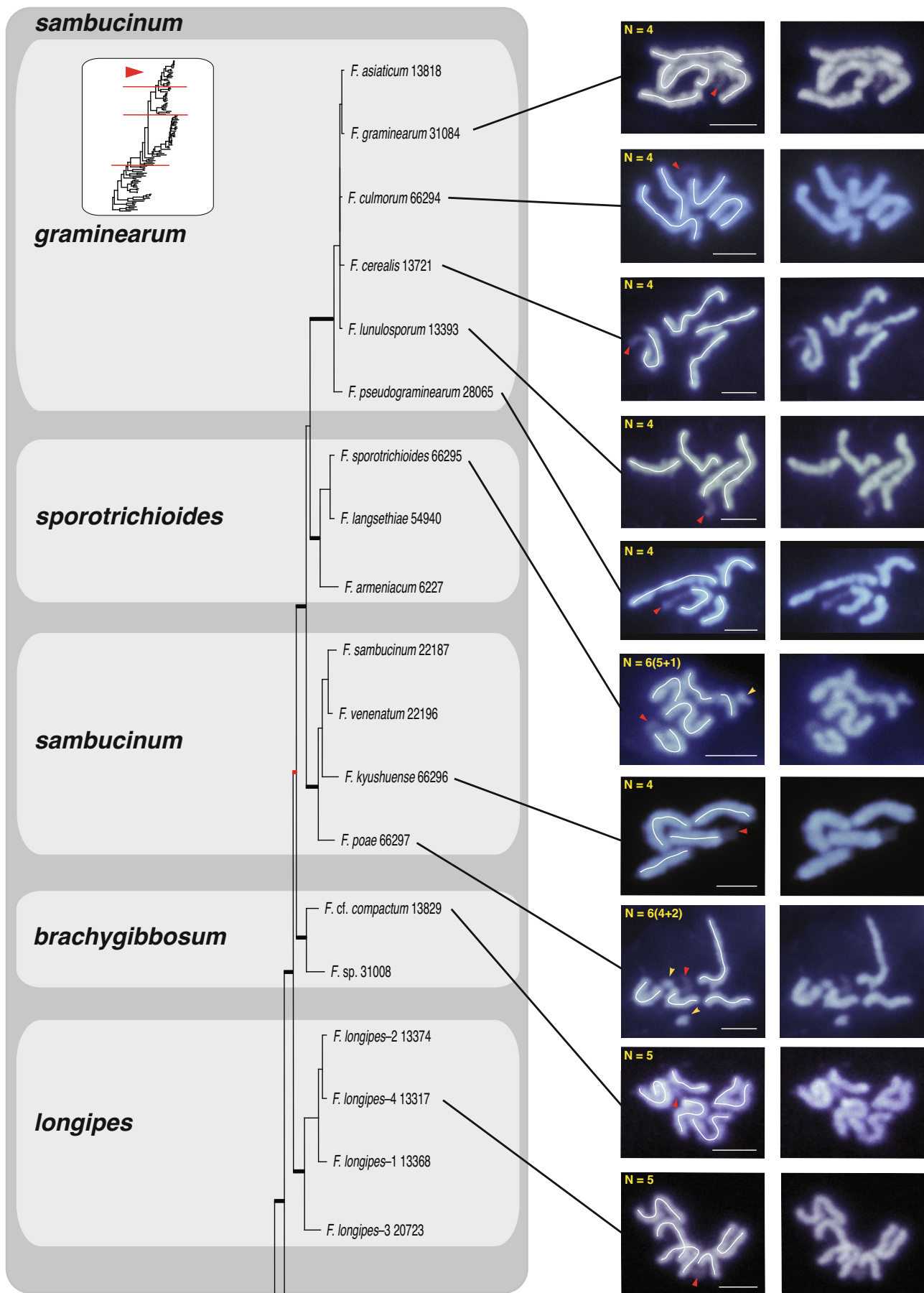
Fig. 1a–d. One of eight most-parsimonious phylograms, 12 982 steps in length, inferred from 3383 bp of aligned partial *RPB1* and *RPB2* sequences from 104 fusaria comprising 20 species complexes. The phylogram was rooted on outgroup sequences of *Neonectria* and *Ilyonectria* based on prior analyses (O'Donnell *et al.* 2013). ARS Culture Collection strains are identified by the 4-5 digit NRRL number. Thickened black nodes received $\geq 90\%$ ML-BS/MP-BS support, whereas the eight nodes in red received $< 70\%$ ML-BS/MP-BS. The chromosome number (CN) traced in the left panel for 31 species representing 11 species complexes was determined by the germ tube burst method and DAPI staining (Taga *et al.* 1998). Putative supernumerary chromosomes in 19 species spanning 11 species complexes are identified by a yellow arrowhead and the number following the + sign. A red arrowhead is used to specify NOR (rDNA), which is identifiable by the protrusion of chromatin from the apex of one of the chromosomes. A green trace line and green arrowheads are used to present an alternative interpretation of the karyotype of *Fusarium buharicum* and *F. sublunatum*. Bar = 2 μ m



1b



1c



1d

chromosomes in *F. subglutinatum* was not due to an increase in genome size. If *F. subglutinatum* was diploid, single nucleotide polymorphisms (SNPs) could exist among homologous chromosomes even if homologous genomic regions had sufficient identity to be assembled into the same contig. Thus, SNPs should be evident in alignments of individual reads to contig sequences; that is, for a segment of the genome with a SNP, half the reads should have one base at the SNP position, while the other half of the reads should have a different base at the same position. However, SNP analysis indicated that the frequencies were similar: 0.028 % in *F. subglutinatum* 13384 and 0.033 % in *F. buharicum* 13371. This finding is consistent with the two fungi having the same ploidy.

To further investigate whether the change in CN in *F. subglutinatum* 13384 was due to diploidization, a qPCR experiment was conducted to assess ploidy of *F. buharicum* and *F. subglutinatum*. After each strain was grown in yeast-malt (YM) broth, the filtered mycelium was lyophilized and then 30 mg of *F. graminearum* 29169 dry weight mycelium was added as an internal normalizing control to 50 mg of each strain (13384 and 13371) as an internal normalizing control. Following genomic DNA extraction, primer efficiency curves showed primer pairs targeting *TEF1* (qTEFf x qTEFr) and *RPB1* (qRPBf x qRPBr) were 97.1 % and 97.2 % efficient, respectively. Primers targeting the *Tri6* gene (efficiency 99.3 %), which is only present in *F. graminearum* 29169, were used as a reference control for normalization to assess fold-changes in gene copy number between strains 13371 and 13384. The geometric mean of the two genes Cq value was then normalized to *Tri6*. The fold change in copy number of *TEF1* and *RPB1* in 13384 relative to 13371 was then calculated as 1.0017 ± 0.08 . Thus, there is no indication of increased ploidy number given that each strain has approximately the same copy number of the two single copy nuclear genes tested.

***Fusarium lateritium* species complex**

The CN of *Fusarium stilboides* 20429, the sole representative of the *F. lateritium* species complex, was 14+1 (Figs 1b, S1b).

***Fusarium nisikadoi* and *F. fujikuroi* species complexes**

The chromosome complement of two strains of *F. nisikadoi*, 25203 and 25308, was determined as 10+1 and 11+1, respectively (Figs 1b, S1b). The closely related *F. fujikuroi* species complex (FFSC) consists of a large number of species with phytopathological and mycotoxigenic relevance. The FFSC is composed of species that cluster in three major clades that coincide with their putative geographic origin and/or the origin of their respective hosts in Africa, Asia and South America (O'Donnell et al. 1998). The CN of the Asian clade *F. fujikuroi* strains 66288 and 66292 was 11+1 (Figs 1b and S1b). The other Asian clade representative, *F. proliferatum* 66289 and 36220, possessed 10+2 and 11+2 chromosomes, respectively (Figs 1b and S1b). Two species in the African clade were karyotyped: *F. verticillioides* 66290 with 10+1 and *F. nygamai* 66291 and 66293 with 12 and 13+2 chromosomes, respectively (Figs 1b, S1b).

***Fusarium heterosporum* species complex**

The CNs of *F. gramineum* 20693 and *F. heterosporum* 20692 were 7 and 7+1, respectively (Figs 1c, S1c).

***Fusarium tricinctum* species complex**

The following five species in this complex were karyotyped: *F. avenaceum* 36374 and 26911 with 8+1 and 8+2 chromosomes, respectively; *F. arthrosporioides* 26416 with 8+3; *F. acuminatum* 28652 and 28449 with 9+1 and 8+1, respectively; *F. tricinctum* 25481 with 8+1 and *Fusarium* sp. 36132 with 9+1 (Figs 1c, S1c).

***Fusarium incarnatum-equiseti* species complex (FIESC)**

The CNs of two unnamed phyloclades in this species-rich complex, FIESC 16-f (NRRL 20425) and FIESC 24-e (NRRL 36255) were 9 and 8+1, respectively (Figs 1c, S1c).

***Fusarium sambucinum* species complex**

Ten species, including representatives of five subclades, were karyotyped within the *F. sambucinum* species complex (Figs 1d, S1d). The CN of *F. longipes*-4 13317 and *F. cf. compactum* 13829 in the *longipes* and *brachygybbsum* subclades, respectively, was five. The chromosome complement of *F. poae* 66297 and *F. kyushuense* 66296 in the *sambucinum* subclade was 4+2 and 4, respectively (Figs 1d, S1d). The CN of *F. sporotrichioides* 66295 in the subclade by the same name was 5+1. Lastly, the following five species in the *graminearum* subclade, also known as the B clade of trichothecene toxin-producing fusaria, possessed four chromosomes (Figs 1d, S1d): *F. pseudograminearum* 28065, *F. lunulosporum* 13393, *F. cerealis* 13721 and 25491, *F. culmorum* 66294, and *F. graminearum* 31084 and 38154. The nucleolar organizing region (NOR) representing the amplified rDNA region was visible as an extension of one of the four chromosomes in all 10 *F. sambucinum* clade species (indicated by red arrowhead, Figs 1d, S1d).

Karyotype reduction

Core CNs in species complexes where two or more karyotypes were obtained were comparable: *ventricosum* (CN = 10–11), *fujikuroi* (CN = 10–12), *tricinctum* and *incarnatum-equiseti* (CN = 8–9), *heterosporum* (CN = 7), and *sambucinum* (CN = 4–5). The latter was the most deeply sampled clade, resulting in the discovery that CNs of species in all five subclades appeared to be fixed: *sporotrichioides*, *brachygybbsum* and *longipes* with CN = 5 and *sambucinum* and *graminearum* with CN = 4. To test if this reduction in karyotype was due to chromosome fusions, genomes retrieved from public repositories were aligned, using MUMmer and Blast2. Large regions of synteny were identified between the genomes of *F. graminearum*, *F. avenaceum*, *Fusarium* sp. FSSC 11 (published as *F. solani*; Coleman et al. 2009) and *F. verticillioides*. (Fig. S2). The left half of chr I of *F. graminearum* showed synteny with the largest chromosome of *F. verticillioides* and the largest contig from the assemblies of *F. avenaceum* isolates FaLH27 and *Fusarium* sp. FSSC 11. The central part of *F. graminearum* chr I showed synteny with parts of chromosomes IV and VIII of *F. verticillioides* and with single contigs of *F. avenaceum* and *Fusarium* sp. FSSC 11. Finally, the distal part of *F. graminearum* chr I was syntenic with chr V of *F. verticillioides*, one contig in *F. avenaceum* and two contigs in *Fusarium* sp. FSSC 11 (Fig. S2). However, no remnants of telomere sequences were detected at the putative chromosomal junctions in *F. graminearum* chr I.

DISCUSSION

We used the GTBM to karyotype 44 strains comprising 33 *Fusarium* species, and these included representatives of 11 species complexes that spanned the phylogenetic breadth of the genus. When viewed within a robust evolutionary framework, karyotype evolution in five closely related clades (*tricinctum* and *incarnatum-equiseti* CN = 8-9, *chlamyosporum* CN = 8 [electrophoretic karyotype reported in Fekete *et al.* 1993], *heterosporum* CN = 7 and *sambucinum* CN = 4-5) appears to have been dominated by a reduction in core CN, consistent with previous reports in *Fusarium* (Ma *et al.* 2010), and the general trend of genome reduction in eukaryotes (Wolf & Koonin 2013). However, a core CN reduction in the sisters of the aforementioned clades was not detected (*lateritium* CN = 14, *nisikadoi* CN = 10-11, *oxysporum* CN = 11 (Ma *et al.* 2010) and *fujikuroi* CN = 10-13); their CNs are comparable to those identified in the three most basal clades in *Fusarium* we sampled (*dimerum* CN = 13, *ventricosum* CN = 10-11 and *solani* CN = 9-12). Given the divergence time estimate for *Fusarium* that places its origin at approximately 83 Mya in the Cretaceous (O'Donnell *et al.* 2013), our limited sampling suggests CN may be relatively stable within most clades with the notable exception of the *F. solani* (CN = 9-12) and *F. buharicum* species complexes (*F. buharicum* CN = 9+1 and *F. sublunatum* CN = 18-20).

We postulated that the two-fold increase in CN observed in *F. sublunatum* might be due to diploidization, but were able to reject this hypothesis based on a comparative genomic analysis and a qPCR experiment that indicated these species share the same copy number of the two genes evaluated. Although the precise mechanism(s) that contributed to the two-fold difference in CN are unknown, they might be elucidated by whole-genome sequencing to sufficient depth that each scaffold corresponds to a whole chromosome as recently done for *F. fujikuroi* (Wiemann *et al.* 2013). To obtain a high quality assembly, SMRT sequencing might be necessary to assemble repetitive sequences (Vanheule *et al.* 2016). Preliminary analyses of in-house sequencing of *F. buharicum* 13371 and *F. sublunatum* 13384 suggests that the overall genome size in both species is ~36 Mb. This is in good agreement with the size of the core genome of most fusaria (Kim *et al.* 2017).

The present study also extends the initial discovery of variable numbers of supernumerary chromosomes in *Fusarium* sp. FSSC 11 (as *F. solani* f. sp. *pisi*) by Miao *et al.* (1991), and the eight fusaria karyotyped electrophoretically by Fekete *et al.* (1993), to four additional fusaria (*F. ventricosum*-1, *F. striatum*, *Fusarium* sp. FSSC 10 and *F. nygamae*). In this regard, putative supernumerary chromosomes were detected in one or more of the fusaria in all 11 clades sampled, but our data suggests they may be less prevalent in the *F. sambucinum* species complex where they were only detected in two of the 10 species karyotyped (i.e., *F. poae* and *F. sporotrichioides*), and none were detected within the *graminearum* subclade. Numerous studies have established that some fungal genomes are composed of core chromosomes, which are stable within a species and contain all functions that allow the organism to complete various aspects of its life-cycle, and additional chromosomes that are not involved in primary metabolism

(summarized in Mehrabi *et al.* 2017: table 1). These additional chromosomes are usually small (< 2 Mb), frequently meiotically unstable, and they often have low gene density and a high number of repetitive sequences (Möller & Stukenbrock 2017). They have been referred to as conditionally dispensable (CD), mini- or B, accessory or supernumerary chromosomes (Covert *et al.* 1998)

In *F. oxysporum* these additional chromosomes were named lineage-specific (LS), because they possess effector genes that determine host specificity (Ma *et al.* 2010). We did not karyotype any representative of the *F. oxysporum* species complex, but whole-genome sequencing of the tomato vascular wilt pathogen, *F. oxysporum* f. sp. *lycopersici*, strain FoI 4287 identified 11 core and four supernumerary or LS chromosomes (Ma *et al.* 2010). The core chromosomes show high similarity among *F. oxysporum* isolates pathogenic to completely different hosts, as well as the putative non-pathogenic strain Fo47 with biocontrol potential (Ma *et al.* 2010). Furthermore, comparison of the tomato pathogen FoI4287 and cucurbit pathogen Forc016 showed that both strains share 11 highly syntenic core chromosomes with >98 % sequence similarity (Van Dam *et al.* 2017). In parallel with FoI4287, the cucurbit strain Forc016 contains three small chromosomes (2.4 Mb, 1.6 Mb and 1.2Mb, respectively) that can be lost without interference with *in vitro* growth. However, transfer of the 2.4 Mb chromosome to Fo47 revealed its role in pathogenicity towards cucumber, melon and watermelon (Van Dam *et al.* 2017). A core and accessory genome were also reported for *F. poae*, where four core chromosomes were highly syntenic with the four chromosomes of *F. graminearum* (Vanheule *et al.* 2016). In addition to these chromosomes, 8 Mb of extra DNA was detected *via* single-molecule real-time (SMRT) sequencing of *F. poae*. In contrast to members of the *F. solani* and *F. oxysporum* species complexes, the CG-content as well as the gene density of this accessory DNA was similar to that in the core genome. However, the accessory DNA of *F. poae* was very rich in transposable elements (25.6 % vs. only 2.1 % in the core genome) and it contained multiple gene duplications.

We reviewed papers reporting karyotypes of fusaria employing classical aceto-carmine, aceto-orcein and HCl-Giemsa staining techniques but they are not discussed in detail here because, with the notable exception of CN = 4 in *F. graminearum* (Howson *et al.* 1963), most of the numbers reported appear to be underestimates. For example, Howson *et al.* (1963) reported CN = 4 in *F. fujikuroi* and *F. stilboides* whereas we discovered CN = 11+1 and 14+1, respectively, in these two species. In contrast, Punithalingam (1972) observed of eight chromosomes in *F. culmorum*, which is an overestimate based on our data, which unambiguously show this species possesses four chromosomes. Following its introduction in the late 1980s, pulsed field gel electrophoresis has been used extensively to karyotype diverse fusaria. Results of the present study match the findings of Fekete *et al.* (1993) who reported karyotypes that are identical to four of the fusaria we typed (i.e. *F. avenaceum* CN = 8, *F. poae* CN = 6, *F. sporotrichioides* CN = 6 and *F. tricinctum* CN = 9). In contrast to the electrophoretic karyotype study by Xu *et al.* (1995), who reported 35 strains representing six species in the *F. fujikuroi* species complex all possessed

12 chromosomes, our data indicate the CN of different strains of two of these species (*F. verticillioides* 66290 and *F. proliferatum* 36220) is 11 and 13, respectively. The CN of 11 in *F. verticillioides* 66290 might be due to loss of chromosome 12, which has been reported to be dispensable and meiotically unstable (Xu & Leslie 1996, Migheli et al. 1993). This chromosome was also absent from the whole genome sequence of *F. verticillioides* 20956 (Ma et al. 2010). Lastly, highly reproducible electrophoretic karyotypes were obtained for 15 VCGs of *F. oxysporum* f. sp. *cubense*, where CN ranged from nine to 14 (Boehm et al. 1994). The wide variation in CN in *F. oxysporum* f. sp. *cubense*, however, is likely due to the polyphyletic origins of this forma specialis (O'Donnell et al. 2000).

The first *Fusarium* comparative genomics study included whole-genome analyses of *F. graminearum*, *F. verticillioides* and *F. oxysporum* (Ma et al. 2010). These authors discovered the core chromosomes of *F. verticillioides* and *F. oxysporum* were highly syntenic, and they reported the four chromosomes of *F. graminearum* were composed of regions syntenic to multiple chromosomes of *F. verticillioides* and *F. oxysporum*. Additional lines of evidence support their hypothesis that the low chromosome number of four in *F. graminearum* and related species in the *sambucinum* subclade resulted from chromosomal fusions in their ancestors. Cuomo et al. (2007) reported that SNP frequencies were elevated and a higher density of genes coding for secreted proteins and genes expressed *in planta* were present at the putative junctions of the ancestral fused chromosomes. These junctions were also shown to contain genes that exhibited lower conservation and expression (Zhao et al. 2014). Moreover, gene clusters involved in specialized metabolism were overrepresented in these non-conserved regions. This finding supports the hypothesis that multiple chromosome fusion events may have occurred during the evolution of the genus, leading to karyotypes as small as CN = 4 in *F. graminearum*, which is one of the lowest observed in filamentous fungi. Integration of whole-genome sequence data from different sequencing platforms offers the promise of complete assemblies where contigs correspond to individual chromosomes with telomeric repeats on both ends as was shown for *F. poae* (Vanheule et al. 2016), *F. fujikuroi* (Wiemann et al. 2013) and *F. subglutinans* and *F. temperatum* (Waalwijk et al. 2017). The CN data presented here should provide a valuable reference for future comparative genomics studies of this agriculturally and medically important genus.

ACKNOWLEDGEMENTS

We are pleased to acknowledge the skilled technical assistance of Gail Doehring, Nathane Orwig, Amy McGovern, Jennifer Teresi, and Ahmed M. Nhmoud in various aspects of this study. Gert H.J. Kema (Wageningen Plant Research) is acknowledged for initiating the research reported here. Mention of trade names or commercial products in this publication is solely for the purpose of providing specific information and does not imply recommendation or endorsement by the U.S. Department of Agriculture. USDA is an equal opportunity provider and employer. CW received financial support from H2020 project MycoKey (project no. 678781).

REFERENCES

- Akamatsu H, Taga M, Kodama M, Johnson R, Otani, H, Kohmoto K (1999) Molecular karyotypes for *Alternaria* plant pathogens known to produce host-specific toxins. *Current Genetics* **35**: 647–656.
- Al-Hatmi AMS, Meis JF, de Hoog GS (2016) *Fusarium*: molecular diversity and intrinsic drug resistance. *PLoS Pathogens* **12**: e1005464
- Aoki T, O'Donnell K (1999) Morphological and molecular characterization of *Fusarium pseudograminearum* sp. nov., formerly recognized as the group 1 population of *F. graminearum*. *Mycologia* **91**: 597–609.
- Aoki T, O'Donnell K, Geiser DM (2014) Systematics of key phytopathogenic *Fusarium* species: current status and future challenges. *Journal of General Plant Pathology* **80**: 189–201.
- Boehm EWA, Ploetz RC, Kistler HC (1994) Statistical analysis of electrophoretic karyotype variation among vegetative compatibility groups of *Fusarium oxysporum* f. sp. *cubense*. *Molecular Plant-Microbe Interactions* **7**: 196–207.
- Brown DW, Lee SH, Kim LH, Ryu JG, Lee S, et al. (2015) Identification of a 12-gene fusaric acid biosynthetic gene cluster in *Fusarium* species through comparative and functional genomics. *Molecular Plant-Microbe Interactions* **28**: 319–332.
- Coleman JJ, Rounsley SD, Rodriguez-Carres M, Kuo A, Wasmann CC, et al. (2009) The genome of *Nectria haematococca*: contribution of supernumerary chromosomes to gene expansion. *PLoS Genetics* **5**: e1000618.
- Covert SF (1998) Supernumerary chromosomes in filamentous fungi. *Current Genetics* **33**: 311–319.
- Cuomo CA, Güldener U, Xu JR, Trail F, Turgeon BG, et al. (2007) The *Fusarium graminearum* genome reveals a link between localized polymorphism and pathogen specialization. *Science* **317**: 1400–1402.
- Dean R, Van Kan JAL, Pretorius ZA, Hammond-Kosack KE, Di Pietro A (2012) The top 10 fungal pathogens in molecular plant pathology. *Molecular Plant Pathology* **13**: 414–430.
- Fekete C, Nagy R, Debets AJM, Hornok L (1993) Electrophoretic karyotypes and gene mapping in eight species of the *Fusarium* sections *Arthrosporiella* and *Sporotrichiella*. *Current Genetics* **24**: 500–504.
- Gale LR, Bryant JD, Calvo S, Giese H, Katan T, et al. (2005) Chromosome complement of the fungal plant pathogen *Fusarium graminearum* based on genetic and physical mapping and cytological observations. *Genetics* **171**: 985–1001.
- Gardes M, Bruns TD (1993) ITS primers with enhanced specificity for basidiomycetes—application to the identification of mycorrhizae and rusts. *Molecular Ecology* **2**: 112–118.
- Geiser DM, del Mar Jiménez-Gasco M, Kang S, Makalowska I, Veeraraghavan N, et al. (2004) FUSARIUM-ID v. 1.0: A DNA sequence database for identifying *Fusarium*. *European Journal of Plant Pathology* **110**: 473–479.
- Geiser DM, Aoki T, Bacon CW, Baker SE, Bhattacharyya MK, et al. (2013) One Fungus, One Name: defining the genus *Fusarium* in a scientifically robust way that preserves longstanding use. *Phytopathology* **103**: 400–408.
- Guarro J (2013) Fusariosis, a complex infection caused by a high diversity of fungal species refractory to treatment. *European Journal of Clinical Microbiology and Infectious Diseases* **32**: 1491–1500.

- Howson WT, McGinnis RC, Gordon WL (1963) Cytological studies on the perfect stages of some species of *Fusarium*. *Canadian Journal of Genetics and Cytology* **5**: 60–64.
- Johnson GD, Araujo GM (1981) A simple method of reducing the fading of immunofluorescence during microscopy. *Journal of Immunological Methods* **43**: 349–350.
- Kim H-S, Proctor RH, Brown DW (2017) Comparative genomic analysis of secondary metabolite gene clusters in 207 isolates of *Fusarium*. *29th Fungal Genetics Conference Abstracts*: 170.
- Laurence MH, Summerell BA, Burgess LW, Liew ECY (2011) *Fusarium burgessii* sp. nov. representing a novel lineage in the genus *Fusarium*. *Fungal Diversity* **49**: 101–112.
- Ma LJ, Van der Does HC, Borkovich KA, Coleman JJ, Daboussi MJ, et al. (2010) Comparative genomics reveals mobile pathogenicity chromosomes in *Fusarium*. *Nature* **464**: 367–373.
- Ma L-J, Geiser DM, Proctor RH, Rooney AP, O'Donnell K, et al. (2013) *Fusarium* pathogenomics. *Annual Review of Microbiology* **67**: 399–416.
- Mahmoud AM, Taga M (2012) Cytological karyotyping and characterization of a 410 kb mini-chromosome in *Nectria haematococca* MPI. *Mycologia* **104**: 845–856.
- Mehrabi R, Taga M, Aghaee M, de Wit PJGM, Kema GHJ (2012) Karyotyping methods for fungi. In: *Plant Fungal Pathogens*. [Methods in Molecular Biology vol; 835.] (Bolton MD, Thomma BPHJ, eds): 591–602. Clifton, NJ: Humana Press.
- Mehrabi R, Gohari AM, Kema GHJ (2017) Karyotype variability in plant-pathogenic fungi. *Annual Review of Phytopathology* **55**: 483–503.
- Miao VP, Covert SF, VanEtten DK (1991) A fungal gene for antibiotic resistance on a dispensable (“B”) chromosome. *Science* **254**: 1773–1776.
- Migheli Q, Berio T, Gullino ML (1993) Electrophoretic karyotypes of *Fusarium* spp. *Experimental Mycology* **17**: 329–337.
- Möller M, Stukenbrock EH (2017) Evolution and genome architecture in fungal plant pathogens. *Nature Reviews Microbiology*: doi.org/10.1038/nrmicro.2017.76
- Munkvold GP (2017) *Fusarium* species and their associated mycotoxins. In: *Mycotoxigenic Fungi: methods and protocols* (Moretti A, Susca A, eds): 51–106. New York: Humana Press.
- Nelson PE, Toussoun TA, Marasas WFO (1983) *Fusarium Species: an illustrated manual for identification*. University Park, PA: Pennsylvania State University Press.
- Nirenberg H (1976) Untersuchungen über die morphologische und biologische Differenzierung in der *Fusarium*-Sektion *Liseola*. *Biologischen Bundesanstalt für Land- und Forstwirtschaft, Berlin-Dahlem* **169**: 1–117.
- O'Donnell K, Kistler HC, Cigelnik E, Ploetz RC (1998) Multiple evolutionary origins of the fungus causing Panama disease of banana: concordant evidence from nuclear and mitochondrial gene genealogies. *Proceedings of the National Academy of Sciences, USA* **95**: 2044–2049.
- O'Donnell K, Rooney AP, Proctor RH, Brown DW, McCormick SP, et al. (2013) Phylogenetic analyses of *RPB1* and *RPB2* support a middle Cretaceous origin for a clade comprising all agriculturally and medically important fusaria. *Fungal Genetics and Biology* **52**: 20–31.
- O'Donnell K, Sutton DA, Fothergill A, McCarthy D, Rinaldi MG, et al. (2008) Molecular phylogenetic diversity, multilocus haplotype nomenclature, and in vitro antifungal resistance within the *Fusarium solani* species complex. *Journal of Clinical Microbiology* **46**: 2477–2490.
- O'Donnell K, Sutton DA, Rinaldi MG, Gueidan C, Sarver BAJ, et al. (2010) Internet-accessible DNA sequence database for identifying fusaria from human and animal infections. *Journal of Clinical Microbiology* **48**: 3708–3718.
- O'Donnell K, Sutton DA, Wiederhold N, Robert VARG, Crous PW, Geiser DM (2016) Veterinary fusarioses within the United States. *Journal of Clinical Microbiology* **54**: 2813–2819.
- O'Donnell K, Ward TJ, Robert VARG, Crous PW, Geiser DM, Kang S (2015) DNA sequence-based identification of *Fusarium*: current status and future directions. *Phytoparasitica* **43**: 583–595.
- Punithalingam E (1972) Cytology of *Fusarium culmorum*. *Transactions of the British Mycological Society* **58**: 225–230.
- Schmittgen TD, Livak KJ (2008) Analyzing real-time PCR data by the comparative CT method. *Nature Protocols* **3**: 1101–1108.
- Schroers H-J, Samuels GJ, Zhang N, Short DPG, Juba J, Geiser DM (2016) Epitypification of *Fusisporium (Fusarium) solani* and its assignment to a common phylogenetic species in the *Fusarium solani* species complex. *Mycologia* **108**: 806–819.
- Shirane N, Masuko M, Hayashi Y (1988) Nuclear behavior and division in germinating conidia of *Botrytis cinerea*. *Phytopathology* **78**: 1627–1630.
- Swofford DL (2003) *PAUP*: phylogenetic analysis using parsimony (and other methods)*. Version 40b10. Sunderland, MA: Sinauer Associates.
- Taga M, Murata M (1994) Visualization of mitotic chromosomes in filamentous fungi by fluorescence staining and fluorescence in situ hybridization. *Chromosoma* **103**: 408–413.
- Taga M, Murata M, Saito H (1998) Comparison of different karyotyping methods in filamentous ascomycetes – a case study of *Nectria haematococca*. *Mycological Research* **102**: 1355–1364.
- Tatusova TA, Madden TL (1999) BLAST 2 Sequences, a new tool for comparing protein and nucleotide sequences. *FEMS Microbiology Letters* **174**: 247–250.
- Taylor JW, Jacobson DJ, Kroken S, Kasuga T, Geiser DM, et al. (2000) Phylogenetic species recognition and species concepts in fungi. *Fungal Genetics and Biology* **31**: 21–32.
- Thomma BPHJ, Seidl MF, Shi-Kunne X, Cook DE, Bolton MD, et al. (2016) Mind the gap: seven reasons to close fragmented genome assemblies. *Fungal Genetics and Biology* **90**: 24–30.
- Tsuchiya D, Taga M (2001) Cytological karyotyping of three *Cochliobolus* spp. by the germ tube burst method. *Phytopathology* **91**: 354–360.
- Tsuchiya D, Taga M (2010) Fluorescence *in situ* hybridization for molecular cytogenetic analysis in filamentous fungi. In: *Molecular and Cell Biology Methods for Fungi* (Sharon A, ed.): 235–257. Clifton, NJ: Humana Press.
- Van Dam P, Fokkens L, Ayukawa Y, van der Gragt M, ter Horst A, et al. (2017) A mobile pathogenicity chromosome in *Fusarium oxysporum* for infection of multiple cucurbit species. *Science Reports* **7**: 9042.
- VanEtten H, Funnell-Baerg D, Wasmann C, McCluskey K (1994) Location of pathogenicity genes on dispensable chromosomes in *Nectria haematococca* MP VI. *Antonie van Leeuwenhoek* **65**: 263–267.
- Vandesompele J, De Preter K, Pattyn F, Poppe B, Van Roy N, et al. (2002) Accurate normalization of real-time quantitative RT-PCR data by geometric averaging of multiple internal control genes. *Genome Biology* **3**: https://doi.org/10.1186/gb-2002-3-7-research0034
- Vanheule A, Audenaert K, Warris S, Van de Geest H, Schijlen E, et al. (2016) Living apart together: crosstalk between the core

- and supernumerary genomes in a fungal plant pathogen. *BMC Genomics* **17**: 670.
- Waalwijk C, Vanheule A, Audenaert K, Zhang H, Warris S, et al. (2017) *Fusarium* in the age of genomics. *Tropical Plant Pathology* **42**: 184–189.
- Wiemann P, Sieber CMK, von Bargen KW, Studt L, Niehaus E-M, et al. (2013) Deciphering the cryptic genome: genome-wide analyses of the rice pathogen *Fusarium fujikuroi* reveal complex regulation of secondary metabolism and novel metabolites. *PLoS Pathogens* **9**: e1003475.
- Wolf YI, Koonin EV (2013) Genome reduction as the dominant mode of evolution. *Bioessays* **35**: 829–837.
- Xu JR, Leslie JF (1996) A genetic map of *Gibberella fujikuroi* mating population A (*Fusarium moniliforme*). *Genetics* **143**: 175–189.
- Xu JR, Yan K, Dickman MB, Leslie JF (1995) Electrophoretic karyotypes distinguish the biological species of *Gibberella fujikuroi* (*Fusarium* section *Liseola*). *Molecular Plant-Microbe Interactions* **8**: 74–84.
- Zhao C, Waalwijk C, de Wit PJGM, Tang D, van der Lee T (2014) Relocation of genes generates non-conserved chromosomal segments in *Fusarium graminearum* that show distinct and co-regulated gene expression patterns. *BMC Genomics* **15**: 191.
- Zhou X, O'Donnell K, Aoki T, Smith JA, Kasson MT, Cao Z-M (2016) Two novel *Fusarium* species that cause canker disease of prickly ash (*Zanthoxylum bungeanum*) in northern China form a novel clade with *Fusarium torreyae*. *Mycologia* **108**: 668–681.
- Zwickl DJ (2006) *Genetic algorithm approaches for the phylogenetic analysis of large biological sequence data sets under the maximum likelihood criterion*. PhD dissertation, University of Texas, Austin.

SUPPLEMENTAL FIGURE LEGENDS

Supplemental Fig. S1a-d. One of two most-parsimonious phylograms, 12 912 steps in length, inferred from 3383 bp of aligned partial *RPB1* and *RPB2* sequences from 104 fusaria comprising 20 species complexes. Sequences of *Neonectria* and *Ilyonectria* were selected as the outgroup for rooting the phylogram following published analyses (O'Donnell et al. 2013). ARS Culture Collection strains are identified by the 4-5 digit NRRL number. Thickened black nodes received ≥ 90 % ML-BS/MP-BS support, whereas the eight nodes in red received < 70 % ML-BS/MP-BS. The chromosome number (CN), determined by the germ tube burst method with DAPI staining (Taga et al. 1998), is traced in the left panel for 31 species comprising 11 species complexes. Putative supernumerary chromosomes in 19 species spanning 11 species complexes are identified by a yellow arrowhead and the number following the + sign. A red arrowhead is used to specify NOR (rDNA), which is identifiable by its characteristic appearance of a chromatin protrusion from the apex of one of the chromosomes. A green trace line is used to identify an alternative interpretation of the karyotype of *Fusarium sublunatum* 13384. Bar = 2 μ m.

Supplemental Fig. S2a. Synteny between chromosome I of *F. graminearum*(CM000574.1) and contigs of *F. avenaceum* isolate FaLH27 (JQGE01000019.1; JQGE01000007.1 and JQGE01000018.1). **S2b.** Synteny between chromosome I of *F. graminearum* (CM000574.1) and *Fusarium* sp. FSSC 11 (formerly known as *F. solani*) isolate 77-13-4 (ACJF01000001.1, ACJF01000006.1; ACJF01000011.1; ACJF01000018.1; ACJF01000004.1). **S2c.** Synteny between chromosome I of *F. graminearum* (CM000574.1) and chromosomes I, IX, IV and V of *F. verticillioides* (accession #s CM000578, CM000585, CM000581 and CM000582, respectively). Alignments were done using BLAST2 (Tatusova & Madden 1999) with an expect threshold arbitrarily set at $1 \times e^{-50}$, to eliminate short syntenic regions (≤ 100 bp).